*J Neurophysiol* 94: 883–895, 2005.
First published February 23, 2005; doi:10.1152/jn.01171.2004.

**Report**

# Countermanding Eye-Head Gaze Shifts in Humans: Marching Orders Are Delivered to the Head First

**Brian D. Corneil and James K. Elsley**

*Department of Physiology and Pharmacology and Psychology, University of Western Ontario, London, Ontario, Canada*

Submitted 11 November 2004; accepted in final form 19 February 2005

**Corneil, Brian D. and James K. Elsley.** Countermanding eye-head gaze shifts in humans: marching orders are delivered to the head first. *J Neurophysiol* 94: 883–895, 2005. First published February 23, 2005; doi:10.1152/jn.01171.2004. The countermanding task requires subjects to cancel a planned movement on appearance of a stop signal, providing insights into response generation and suppression. Here, we studied human eye-head gaze shifts in a countermanding task with targets located beyond the horizontal oculomotor range. Consistent with head-restrained saccadic countermanding studies, the proportion of gaze shifts on STOP trials increased the longer the stop signal was delayed after target presentation, and gaze shift stop-signal reaction times (SSRTs: a derived statistic measuring how long it takes to cancel a movement) averaged ~120 ms across seven subjects. We also observed a marked proportion of trials (13% of all STOP trials) during which gaze remained stable but the head moved toward the target. Such head movements were more common at intermediate stop signal delays. We never observed the converse sequence wherein gaze moved while the head remained stable. SSRTs for head movements averaged ~190 ms or ~70–75 ms longer than gaze SSRTs. Although our findings are inconsistent with a single race to threshold as proposed for controlling saccadic eye movements, movement parameters on STOP trials attested to interactions consistent with a race model architecture. To explain our data, we tested two extensions to the saccadic race model. The first assumed that gaze shifts and head movements are controlled by parallel but independent races. The second model assumed that gaze shifts and head movements are controlled by a single race, preceded by terminal ballistic intervals not under inhibitory control, and that the head-movement branch is activated at a lower threshold. Although simulations of both models produced acceptable fits to the empirical data, we favor the second alternative as it is more parsimonious with recent findings in the oculomotor system. Using the second model, estimates for gaze and head ballistic intervals were ~25 and 90 ms, respectively, consistent with the known physiology of the final motor paths. Further, the threshold of the head movement branch was estimated to be 85% of that required to activate gaze shifts. From these results, we conclude that a commitment to a head movement is made in advance of gaze shifts and that the comparative SSRT differences result primarily from biomechanical differences inherent to eye and head motion.

## INTRODUCTION

Eye-head gaze shifts, which rapidly change the line of sight via coordinated eye-head movements, are a model system for understanding how the brain controls multi-segmental motion. Like arm movements, eye-head gaze shifts are a form of motor coordination in which movement of a controlled variable, in this case the line of sight, results from the coordinated motion of multiple underlying segments. Unlike arm movements, many of the areas involved in the latter stages of movement generation are within the brain stem and accessible to conventional neurophysiology. Close consideration of the neural mechanisms controlling eye-head gaze shifts may reveal principles that generalize to other multi-segmental motor systems.

Neurophysiological studies have suggested that high levels of activity within the superior colliculus (SC) encode the desired gaze shift rather than the underlying eye or head components (Freedman and Sparks 1997; Freedman et al. 1996; Klier et al. 2001). Other results, predicated on electromyographic (EMG) activity recorded directly from neck muscles (Corneil et al. 2002a,b, 2004), support a more nuanced dual-threshold hypothesis whereby two thresholds dictate the SC contribution to orienting: a higher one surpassed when initiating a gaze shift and a lower threshold surpassed when initiating only a head movement (Galiana and Guitton 1992). Presumably by controlling levels of neural activity relative to these two thresholds, the CNS can "hedge its bets" by initiating an orienting head movement while deciding on a contextually appropriate course of action for the gaze axis.

The goal of this study is to test behavioral predictions arising from this dual-threshold hypothesis. More specifically if neural activity accumulates only beyond the lower threshold, there should be behavioral scenarios wherein the head moves while gaze remains stable. To test this prediction, we study how humans countermand eye-head gaze shifts. The countermanding task (Logan and Cowan 1984) captures the ability to rapidly alter a course of action based on sudden environmental change. Depending on the timing of the task (i.e., the interval between the instructed movement signal and a *stop signal* instructing movement suppression), subjects will either respond or not. The countermanding task comes with a rich psychophysical history (Logan 1994) that has successfully modeled performance as a race to threshold between a GO process controlling response generation and a STOP process controlling response suppression; the outcome of this race determines the behavior on a given trial (Fig. 1*A*). Moreover, the advent of a saccadic version of the countermanding task made possible neurophysiological studies of response control (Hanes et al. 1998; Ito et al. 2003; Paré and Hanes 2003; Stuphorn et al. 2000). In particular, patterns of neural activity in both the frontal eye fields (Hanes and Schall 1996; Hanes et al. 1998) and SC (Paré and Hanes 2003) of head-restrained monkeys support the notion of a race to a single threshold causal to the ensuing behavior. Here, we demonstrate patterns

Address for reprint requests and other correspondence: B. D. Corneil, Centre for Brain and Mind, Robarts Research Institute, London, Ontario N6A 5K8, Canada (E-mail: bcorneil@uwo.ca).

The costs of publication of this article were defrayed in part by the payment of page charges. The article must therefore be hereby marked "*advertisement*" in accordance with 18 U.S.C. Section 1734 solely to indicate this fact.

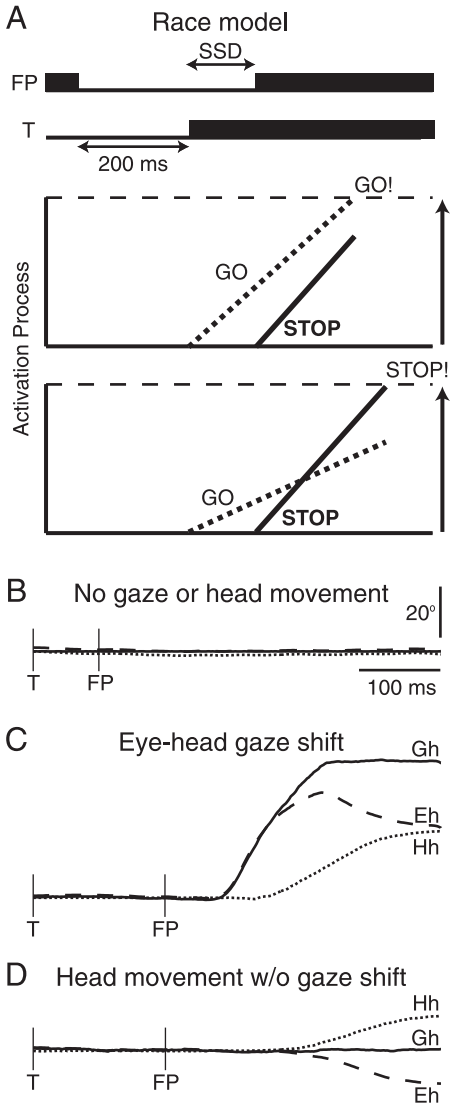


FIG. 1. *A*: depiction of events and race model on STOP trials. The fixation point (FP) disappears for 200 ms before target (T) presentation. The FP reappears at a stop-signal delay (SSD) after target presentation, signaling that the gaze shift is to be cancelled. A race model for control of head-restrained saccades proposes that the accumulation of 2 processes to a threshold, a GO and STOP process, control response generation or suppression, respectively. Depending on the SSD and the rate of rise of these processes, the movement is either generated or successfully withheld. *B–D*: representative examples of horizontal eye (Eh), head (Hh), and gaze (Gh) traces during the 3 response patterns observed on STOP trials, aligned on T presentation. Upward deflections denote rightward movements. All examples come from *s6,* generated when the T was presented 60° right. The SSD was 80 ms in *B* and 160 ms in *C* and *D*. Scale bars in *B* apply to *C* and *D* as well.

of eye-head coordination and gaze shifts that are inconsistent with a simple single race to gaze-shifting threshold but supportive of the notion that head movements are initiated in advance of gaze shifts.

## METHODS

Seven subjects (2 female, 5 males; age range: 22–32 yr) participated after providing their informed written consent. Subjects reported no history of neurological or musculoskeletal disorders, and all had normal or corrected-to-normal vision. Experimental procedures were approved by the University Research Ethics Board for Health Science Research at the University of Western Ontario in accordance with the ethical standards laid down in the 1964 Declaration of Helsinki. Two subjects (*s1* and *s2*, the authors) were knowledgeable about the specific goals of the experiment, and another subject (*s5*) was knowledgeable about the general goals of the study. The remaining subjects were naïve regarding the goals of the experiments. Subjects were not preselected for head-movement propensity. Subjects were instructed beforehand on the nature of the countermanding task (see following text) but were not given any feedback during the experiment. All subjects generated qualitatively similar patterns of eye, head, and gaze movements.

Subjects were seated upright in a straight-back chair in a dark experimental room. The room was compartmentalized by a double layer of thick dark curtains that spanned from floor to ceiling, attenuating the residual illumination given off by the experimental equipment. Background light during the experimental sessions was measured to be $<0.01$ cd/m$^2$ (Minolta CS-100 chromameter). The visual stimuli consisted of three red light-emitting diodes (LEDs; 110 cd/m$^2$, CIEx = 0.642; CIEy = 0.358) embedded within boxes mounted on wooden stands positioned 1.2 m in front of the subject. All LEDs were elevated 1.2 m off the ground to lie on the horizontal meridian from the subject's perspective. One LED was positioned directly in front of the subject to serve as the central fixation point (FP). Two target LEDs were fixed at a radial angle of 60° to the left or right of the FP.

### *Countermanding task*

Subjects performed a countermanding task in which control and STOP trials were intermixed. Both trial types started with the illumination of the central FP for an interval selected randomly between values of 1,000, 1,166, 1,333, and 1,500 ms. The FP was then extinguished for 200 ms, followed by target presentation for 1,000 ms. Our logic for incorporating the 200-ms gap prior to target onset was based on a previous report (Corneil and Munoz 1999) wherein there was an appreciable incidence of head movements without gaze shifts on gap trials, possibly consequent to increased motor preparation after FP disappearance (Dorris and Munoz 1995). On control trials, the subjects simply had to look to the target. On STOP trials, the stop signal consisted of reappearance of the central FP (Fig. 1*A*), and subjects were instructed to not look to the target when it reappeared. The reilluminated FP remained on for as long as the target, after which both were extinguished followed by an inter-trial interval of 500–1,000 ms.

The stop-signal delay (SSD) measures the time from target presentation to FP reappearance on STOP trials (Fig. 1*A*). In these experiments, six SSDs ranged from 0 to 200 ms in 40-ms steps. All subjects completed at least three blocks of 200 trials each. Within each block, 70% of all trials were control trials, and the remaining 30% were STOP trials. All variations (trial type, target direction, SSD) were interleaved pseudorandomly by a customized LABVIEW program downloaded onto a PXI box (National Instruments), which controlled the experiment in real time. All subjects contributed $\geq$420 control trials and 180 STOP trials, the latter being split equally among the six SSDs.

Subjects performed a series of practice trials before the experimental data were collected. Subjects were instructed to look as quickly and as accurately to the presented target with whatever combination of eye and head movements they desired but to try not to move when the stop signal reappeared.

### *Data collection and analysis*

Horizontal eye movements were measured using bi-temporal DC electrooculography (EOG) and were filtered and amplified with a P122 AC/DC preamplifier (Grass Instruments). Horizontal head rotation was measured by having subjects wear a baseball helmet attached to a low-torque potentiometer that was fitted into a metal bar anchored

to a solid desk behind the subject. The potentiometer signal was first calibrated to known angles of rotation. Subjects were then asked to maintain fixation on the central FP while they turned their heads. The gain of the EOG signal was adjusted to be equal and opposite that of the potentiometer signal. Horizontal eye and head movements were filtered (100 Hz, low-pass), amplified, and digitized at a rate of 500 Hz onto the PXI box. Digitized data were then transferred to a PC computer, and subsequent off-line analyses were performed using customized Matlab (the Mathworks) programs. Horizontal gaze (eye-in-space) position was constructed off-line by adding eye and head signals. Eye, head, and gaze movements were analyzed via a customized Matlab Graphical User Interface. Movement onsets and offsets were identified by an automarking program, which detected when crossings of velocity thresholds (50°/s for eye and gaze, 25°/s for head; velocities were differentiated from position traces and filtered with a low-pass Butterworth filter with fs/fc = 17). These automarks were used as guides for the placement of interactive marks by a data analyst that were verified by a second analyst to check for errors and ensure consistency. Movement reaction time (RT), duration, and amplitude were calculated and saved for further analyses. Trials were classified as anticipatory and were excluded from analysis if gaze or head RTs were <80 ms (Corneil and Munoz 1996) or >800 ms due to lack of subject alertness. Less than 1% of all trials was excluded with these two criteria.

We confirmed that target location had no consistent effect across our sample on gaze shift or head movement RTs for control trials ($P = 0.47$ for gaze RTs; $P = 0.16$ for head RTs, Wilcoxon signed-rank test) or on the proportion of STOP trials in which a gaze or head movement was made ($P > 0.55$). All data were subsequently pooled across target location.

## RESULTS

### *Patterns of eye-head movement on STOP trials*

Subjects commonly produced three sequences of eye-head movements on STOP trials: they successfully canceled their gaze shift without moving the eyes or head (Fig. 1*B*), looked to the target via a coordinated eye-head gaze shift (Fig. 1*C*), or generated a sequence wherein the head moved in the direction of the target but gaze remained stable due to a compensatory eye movement in the opposite direction (Fig. 1*D*).

We first quantified the frequency of these three movement sequences, pooled across all SSDs (Table 1). A number of points deserve emphasis. First, all subjects generated all three sequences at appreciable frequencies, with the percentage of canceled gaze shifts ranging from 51 to 86% (mean: 68%). Second, there was a higher incidence of head movements on STOP trials (mean: 44%, range: 20–65%) than gaze movements (mean: 32%, range: 14–49%). This occurred because of STOP trials in which the head moved toward the target while gaze remained stable (i.e., Fig. 1*D*). Such a movement sequence occurred in all subjects on 13% of all STOP trials (range: 6.2–19%), or at a rate approximately one-third that of noncanceled gaze shifts. Third, we very rarely observed examples in which gaze remained stable while the head moved away from the target (0.8% of all STOP trials). Fourth, we never observed incidences in which gaze moved to the target while the head remained stable (not shown in Table 1), likely because our targets lay beyond the oculomotor range.

Next, we investigated the RTs of eye and head movements and gaze shifts across each movement class. RTs for all components of eye-head gaze shifts tended to be smaller when made during STOP versus control trials; however, we defer this analysis until a later section investigating the validity of the assumptions about the race model.

Head-movement RTs depended significantly on the context in which they were made, being shortest when made in conjunction with noncanceled gaze shifts on STOP trials, longer when not accompanied by gaze shifts during STOP trials, and longer still when accompanying gaze shifts during control trials [Table 1 and Fig. 2A; 1-way repeated-measures ANOVA, $F(1,2,12) = 8.72$, $P < 0.005$; head RTs during control trials were significantly longer ($P < 0.05$) than those accompanying gaze shifts on STOP trials; corrected Wilcoxon signed-rank test]. We also investigated the coupling of eye and head movements during gaze shifts and found a tight correlation between eye and head RTs for eye-head gaze shifts made during both control and STOP trials (Fig. 2*B*; $P < 0.001$ and $r^2 > 0.62$ for linear regressions between eye and head RT during both control and STOP trials; eye and gaze onsets are synchronous because rapid, noncompensatory eye movements initiate gaze shifts). This analysis was done only for eye-head gaze shifts in control or STOP trials, as the compensatory eye movement made during STOP trials in which the head moved served to stabilize, not reposition, gaze. Finally, we also found that the relative timing of eye and head movements within gaze shifts differed across control and STOP trials, such that the onset of eye motion led head motion more in control versus STOP trials (Fig. 2*C*;

TABLE 1. *Response sequence probabilities on STOP trials, metrics of head movements without gaze shifts, and head-movement reaction times within various contexts for all subjects*

| | | Response Probability on STOP Trials | | | Head Movements Without Gaze Shifts | | | | Head-Movement Reaction Times, ms | | |
|---|---|---|---|---|---|---|---|---|---|---|---|
| | | | | | | | | | STOP Trials | | |
| Subject | No. of STOP Trials | No gaze shift | Gaze shift | Head movement | Probability | Amplitude, ° | *P* (wrong dir) | Percentage corrected | With gaze shifts | No gaze shifts | Control trials |
| *s1* | 175 | 0.51 (90) | 0.49 (85) | 0.58 (102) | 0.097 (17) | 8.5 ± 4.2 | 0.017 (3) | 86 | 253 ± 42 | 258 ± 44 | 257 ± 39 |
| *s2* | 178 | 0.80 (142) | 0.20 (36) | 0.31 (56) | 0.11 (20) | 5.1 ± 3.2 | 0 (0) | 81 | 331 ± 71 | 348 ± 67 | 350 ± 48 |
| *s3* | 175 | 0.54 (94) | 0.46 (81) | 0.65 (113) | 0.19 (33) | 11.1 ± 9.0 | 0.022 (4) | 63 | 250 ± 34 | 247 ± 33 | 252 ± 38 |
| *s4* | 178 | 0.86 (153) | 0.14 (25) | 0.20 (36) | 0.062 (11) | 3.7 ± 3.0 | 0 (0) | 18 | 328 ± 59 | 333 ± 66 | 355 ± 57 |
| *s5* | 189 | 0.63 (120) | 0.37 (69) | 0.47 (89) | 0.11 (20) | 7.0 ± 4.6 | 0.005 (1) | 46 | 285 ± 55 | 306 ± 53 | 316 ± 55 |
| *s6* | 190 | 0.81 (153) | 0.19 (37) | 0.34 (65) | 0.15 (28) | 5.5 ± 3.5 | 0 (0) | 0 | 304 ± 61 | 317 ± 61 | 356 ± 72 |
| *s7* | 192 | 0.65 (125) | 0.35 (67) | 0.53 (102) | 0.18 (35) | 6.7 ± 4.9 | 0.01 (2) | 47 | 304 ± 87 | 332 ± 55 | 328 ± 76 |
| Mean | | 0.68 | 0.32 | 0.44 | 0.13 | 6.8 ± 2.4 | 0.008 | 48.7 | 293 ± 33 | 306 ± 39 | 317 ± 44 |

All *P* values followed by the number of observations. Amplitudes are given as means ± SD

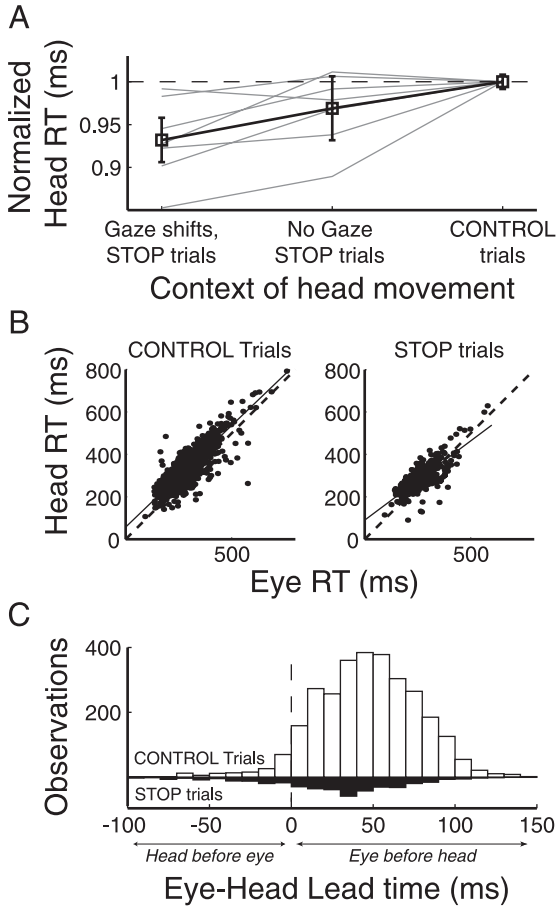


FIG. 2. Reaction times (RTs) in countermanding task. *A*: normalized RTs for head movements made in various contexts, either as part of a noncanceled gaze shift on STOP trials, as the movement sequence on STOP trials when gaze remained stable or on control trials. All RT data normalized to the mean head RT on control trials (horizontal dashed line). Each thin gray line represents data from 1 subject, and the thick black lines and squares represents the mean across the population. Error bars represent SE. *B*: head-movement RTs plotted as a function of eye-movement RTs for gaze shifts made during control or STOP trials. Each dot represents data from a single trial pooled across all gaze shifts. Dashed diagonal lines represent lines of unity; solid lines represent regression lines. *C*: eye-head lead time, for gaze shifts made during control (upward empty histograms) or STOP (lower filled histograms) trials, pooled across all gaze shifts.

mean eye-head lead time in 2,971 control trials = 45.7 ± 34.4 ms; in 399 STOP trials = 24.6 ± 43.5 ms; *t*-test $P < 10^{-5}$).

We also investigated the amplitudes of both head movements and gaze shifts during these various movement sequences. Note that we could only quantify movements occurring within 1,000 ms after target onset, as data recording on each trial ceased at this point. For STOP trials in which neither a gaze shift nor head movement occurred (e.g., Fig. 1*B*), subjects clearly inhibited all target-directed movements and on-line examination showed no tendency for subjects to glance to the target in the inter-trial interval.

The amplitudes of noncanceled gaze shifts and head movements made during STOP trials were significantly less than those made during control trials (control gaze amplitudes = 58.5 ± 7.5°; STOP gaze amplitudes = 45.5 ± 16.6°. *t*-test $P < 10^{-5}$; control head amplitudes during gaze shifts = 38.8 ± 15.6°; STOP head amplitudes during noncanceled gaze shifts = 31.6 ± 14.7°. *t*-test $P < 10^{-5}$). These amplitude differences factor into considerations of race model assumptions and will be discussed in a later section. Despite these amplitude differences, the ratio of the gaze shift accounted for by the head movement was not significantly different for control versus STOP trials (head movement contribution as percentage of total gaze shift; control: 53.8 ± 21.4%; STOP: 56.0 ± 26.3%. *t*-test $P = 0.06$).

Subjects also tended to correct for gaze and/or head movements made during STOP trials, although there were idiosyncratic differences. For noncanceled gaze shifts on STOP trials (e.g., Fig. 1*C*), subjects almost always (97% of the time) generated corrective gaze shifts back to center, accounting for 98.3% of the amplitude of the initial gaze shift. During these corrective gaze shifts, the head also displayed a corrective movement back to center on average 97% of the time in six subjects but only 21% of the time in *subject s6*. We could not analyze the full amplitude of this corrective head movement because it was frequently in-flight 1,000 ms after target onset.

We also investigated the amplitudes of head movement made in STOP trials while gaze remained stable (e.g., Fig. 1*D*) and found that although these amplitudes were modest (mean = 6.8 ± 2.7°; Table 1), they frequently exceeded 10° (25% of the time), and occasionally exceeded 25°. After these head movements, idiosyncratic strategies were apparent: some subjects almost always generated corrective head movements during the 1,000-ms window after target onset (*s1* and *s2*), whereas others did not or did so only rarely (*s4* and *s6*; Table 1). While subjects were given no specific instructions on what to do if they moved during STOP trials, other than not to be concerned about mistakes, they all prepared for the next trial during the inter-trial interval.

We also correlated the size of gaze shifts and head movements on STOP trials to the stop signal delay. Noncanceled movements on STOP trials (be they gaze shifts or head movements with or without gaze shifts) tended to be larger for longer SSDs (Fig. 3; all linear regressions significant at $P < 0.05$. On a per-subject basis, slopes of the linear regression between movement amplitude and SSD were skewed to positive values; $P < 0.05$, 1-way *t*-test). This tradeoff between SSD and movement amplitude is consistent with the STOP process being able to arrest movements in mid-flight even though the

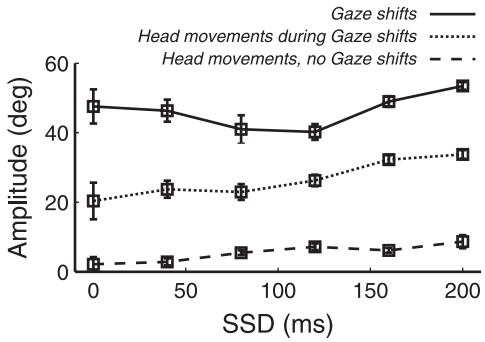


FIG. 3. Noncanceled movement amplitudes on STOP trials as function of SSD. Three movements are represented: noncanceled gaze shifts (—), head movements during noncanceled gaze shifts (· · ·), and head movements made while gaze remained stable (- - -). Data pooled across all subjects and directions; □, mean movement amplitude at each SSD. Error bars represent SE. Note that error bars are largest for the smallest SSDs, as these generally had the fewest observations. Correlations between movement amplitude and SSD were significant for all 3 movements, and all least-square regression lines had positive slopes.

GO process already "won" the race determining movement initiation.

### *Behavioral estimates of gaze shift and head movement cancellation*

Given that the head and gaze showed a differential propensity to move on STOP trials, we were able to construct two inhibition functions expressing response probability across SSDs: one for gaze shift responses and one for head movement responses (made either with or without gaze shifts). These inhibition functions are shown in Fig. 4. Consistent with previous studies, the probability of a response, be it a gaze shift or a head movement, increased with longer SSDs. Importantly, for all subjects, head movement inhibition functions were shifted left compared with gaze shift inhibition functions, implying that there was a greater probability of observing a head movement at a particular SSD. This occurred because of head-movement responses without gaze shifts. The difference between head and gaze inhibition functions expresses the probability of head-movement responses without gaze shifts (Fig. 4, - - -), and a one-way ANOVA of the probability of this response type across SSD demonstrated that such responses were more common at the intermediate SSDs [$F(1,5) = 5.28$; $P < 0.001$; post hoc Bonferroni corrected $t$-test revealed that movements were significantly ($P < 0.05$) more common at the 4th and 5th SSD vs. the 1st and 2nd SSD].

For each subject, we obtained estimates of the SSRT for both head movements and gaze shifts. Briefly, the SSRT is a derived parameter that expresses the amount of time required to cancel a planned movement. Calculating this parameter via the integration method (Logan 1994) requires both the inhibition function from STOP trials and the cumulative RT distribution functions (CDF) from control trials. The SSRT is estimated at each SSD by finding the $P$(response) from the inhibition function, finding the RT from the control CDF corresponding to this $P$ value, and subtracting the SSD (Logan 1994). SSRTs can therefore be calculated at each SSD, leading to a distribution [as suggested in (Logan 1994), we only used $P$(response) values between 0.1 and 0.9]. Gaze and head SSRTs determined by this method are contrasted in Fig. 5*A*. Across all subjects, the head SSRT was significantly longer than the gaze SSRT (mean head SSRT = 200 ± 15 ms; mean gaze SSRT = 123 ± 19 ms; difference = 77 ± 18 ms; Wilcoxon signed-rank test, $P = 0.01$), implying that it takes ~75 ms longer to cancel a planned head movement than a planned gaze shift.

SSRTs can also be estimated using the mean of the inhibition function after converting it to a probability density function. This mean is then subtracted from the mean of the control-trial RT distribution. When we employed this mean method, using a rescaling factor for the value of $p_i$ as suggested in Logan (1994) because $P$(response) did not always range between 0 and 1, the estimated gaze SSRTs equaled 119 ± 19 ms. Head SSRTs derived by this method equaled 190 ± 26 ms. Gaze and head SSRTs derived from the mean method are contrasted in Fig. 5*B*. Across all subjects, head SSRTs determined by the mean method were 70 ± 13 ms longer than gaze SSRTs (Wilcoxon signed-rank test, $P = 0.01$).

The integration and mean methods of estimating SSRTs yielded relatively consistent results on a per subject basis, although there was some scatter particularly for gaze SSRTs (Fig. 5*C*; Table 3). The integration method tended to give slightly higher SSRT estimates [differences of SSRTs determined by integration or mean methods, gaze: 3.7 ± 26.8 ms (range: −30 to 53 ms; positive values imply integration method yielded larger results); head: 10.6 ± 17.6 ms (range: −11 to 38 ms)], but these differences did not reach significance (Wilcoxon signed-rank test comparing estimates of gaze SSRTs, $P > 0.9$; for head SSRTs, $P = 0.15$).

Next, we determined how dependent the comparative SSRTs were on the occurrence of head movements without gaze shifts

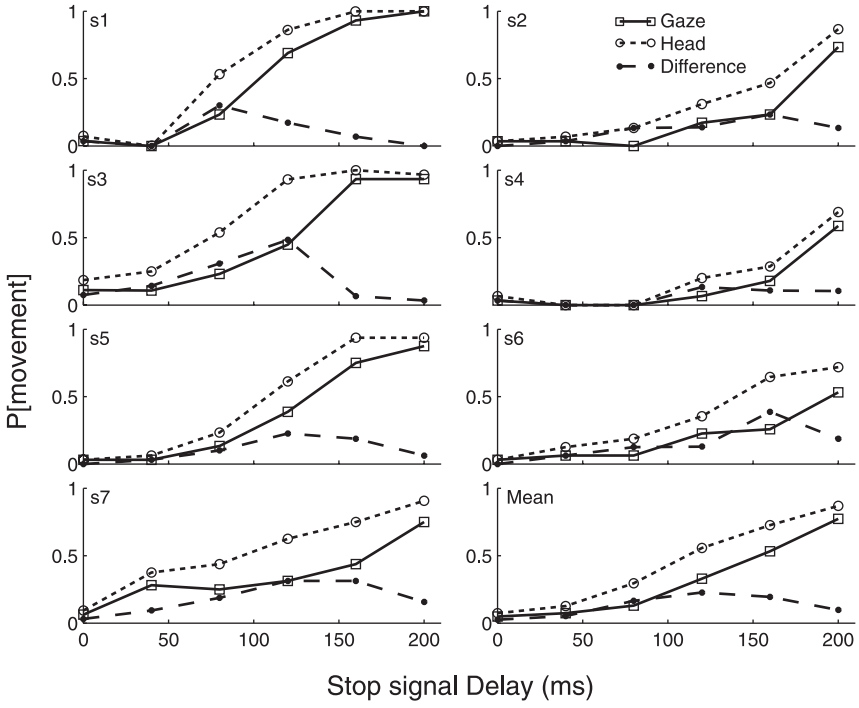


FIG. 4. Inhibition functions, plotting probability of gaze shifts (—) or head movements (either with or without gaze shifts; · · · ) on STOP trials as a function of SSD for all subjects and sample mean. - - -, the difference between the head and gaze inhibition functions.

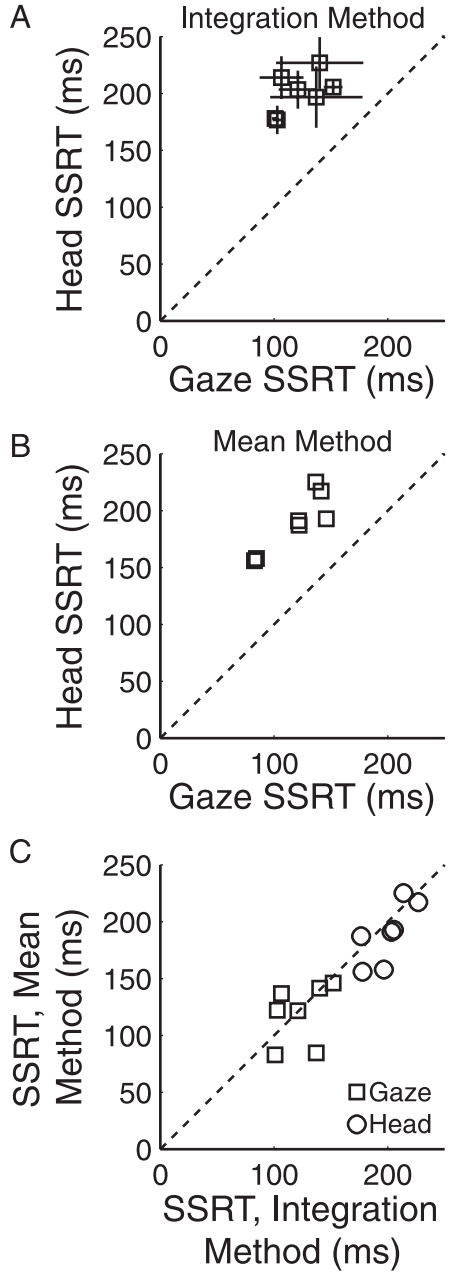


FIG. 5. Comparison of the gaze and head stop-signal reaction times (SSRTs) calculated for each subject, using either the integration method (A; vertical and horizontal lines represent SD) or the mean method (*B*). See text for details. *C*: comparison of gaze (squares) and head (circles) SSRTs derived via the mean or integration method. Each square/circle represents data from 1 subject.

on STOP trials. To answer this question, we repeated our calculation of head SSRTs after excluding STOP trials in which the head moved but gaze remained stable. Because head movements always accompanied gaze shifts on STOP trials, in essence we calculated SSRTs using the gaze inhibition function from STOP trials and the head CDFs from control trials. Head SSRTs derived via the integration method equaled 173 ± 14 ms versus 164 ± 29 ms derived via the mean method ($P = 0.9$). Both of these derived head SSRTs were significantly longer than respective gaze SSRTs by ~50 ms ($P = 0.01$). Our conclusion that it takes longer to cancel a planned head movement therefore does not depend on the presence of head movements on STOP trials without gaze shifts.

### *Tests of the race model*

The race model assumes that the GO and STOP processes are stochastically independent. This assumption can be tested by comparing movement amplitudes from control trials to noncanceled movements made on STOP trials: independence between GO and STOP processes should mean that movement amplitudes in control and STOP trials should be the same. While we have already presented evidence demonstrating that gaze shifts and head movements are attenuated when made during STOP trials (Fig. 3), we do not feel that this necessarily invalidates the independence assumption of the race model. Other groups have reported that amplitudes of noncanceled saccades on STOP trials are less than for control trials (Colonius et al. 2001; Ozyurt et al. 2003; Paré and Hanes 2003), presumably because the STOP process is able to arrest a movement in mid-flight even if movement initiation, determined by when the GO process reaches threshold, is unaffected by the presence of the STOP process. Considering the 60° target eccentricity employed in this study, it is reasonable to assume that the STOP process is able to stop on-going movements in mid-flight. This notion is supported by the resemblance of the movement sequences on STOP trials reported here to movements made in a competitive task where subjects had to orient to a task in the presence of a distractor (Corneil and Munoz 1999; Corneil et al. 1999). When moving erroneously to the distractor, the eyes and head accelerate on an initial trajectory typical of a much larger movement, even though its amplitude was truncated. Thus we do not believe that comparisons of movement amplitude assess the independence assumption of the race model for large-eccentricity movements.

Another test of the independence assumption can be made by determining how well the race model predicts RTs of movements made in noncanceled STOP trials (Logan 1994). The race model dictates that noncanceled movements on STOP trials are produced because the GO process finished before the STOP process. Accordingly, RTs from control trials can be used to predict RTs on noncanceled STOP trials by examining those movements that would have been produced even if the stop signal had been presented. To derive this prediction, for each subject and each SSD, we selected the subset of movements in control trials that had RTs less than the sum of the SSD plus the estimated SSRT (Fig. 6*A*). Using the SSRT estimated via the integration method (SSRTs derived via the mean method gave equivalent results), we found that the median gaze shift RT for noncanceled STOP trials (10 trials minimum) exceeded estimated gaze shift RT from control trials by only 3.7% (mean difference = 8 ms). This difference was significant in 20% (3 of 15) of comparisons but in only 9% (1 of 11) of comparisons with >15 STOP trials (for each subject, there were >15 noncanceled STOP trials at the longer SSDs). The median head movement RT for noncanceled STOP trials exceeded estimated head movement RT from control trials by 2.7% (mean difference = 6 ms). This difference was significant in 9% (2 of 22) of comparisons but in none with >15 STOP trials.

A third test of the race model can be performed by examining how RTs of noncanceled movements change with the SSD: the STOP process should eliminate less of the upper tail of

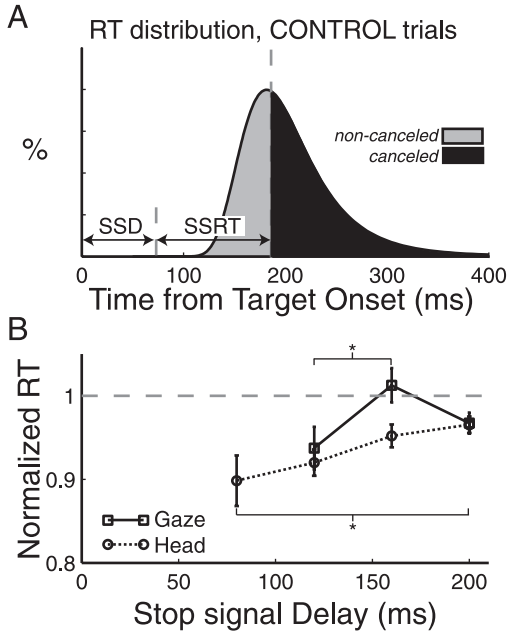


FIG. 6. *A*: depiction of how the race model can be used to predict RTs of noncanceled movements at a given SSD. The RT distribution from control trials can be subdivided into a portion that would or would not have been canceled, had the STOP signal been presented, by the sum of the predetermined SSRT and the given SSD. Those movements falling into the noncanceled portion predict the RTs of noncanceled movements at that SSD. *B*: normalized RTs of noncanceled gaze shifts (□) and head movements (○) as a function of SSD. RTs normalized to the mean of RT from control trials (- - -). Data pooled across all subjects. Consistent with the race model, RTs of noncanceled movements increased for longer SSDs. * and XXX, observations that were significantly different using post hoc Bonferroni corrected *t*-test, $P < 0.05$.

the control RT distribution for longer SSDs (i.e., imagine a longer SSD in Fig. 6*A*). As a result, the RTs of noncanceled movements on STOP trials should be longer for longer SSDs. This prediction was also borne out: both gaze shift and head movement RTs tended to be longer for longer SSDs [Fig. 6*B*; 1-way ANOVA of normalized reaction times across SSD, gaze RTs: $F(2,345) = 3.57$, $P$ 0.03; head RTs: $F(3,517) = 3.57$, $P = 0.02$].

We conclude from these behavioral analyses that there was no large violation of the assumption of independence between GO and STOP processes for the initiation of either gaze shifts or head movements.

### *Modeling the countermanding of eye-head gaze shifts using maximum likelihood techniques*

In this section, we suggest two alternative extensions to the race model to gain a further understanding of plausible neural circuitry that could underlie the observed behavior. These modeling efforts utilize a maximum likelihood technique presented recently by Kornylo and colleagues (2003). The first model (Fig. 7*A*, *model 1*) simply assumes that gaze shifts and head movements are controlled by the outcome of parallel races, each endowed with independent GO and STOP processes. This architecture is analogous to architecture thought to underlie the countermanding of eye and arm movements (Boucher et al. 2004; Logan and Irwin 2000; Mirabella et al. 2004). In this model, each of four processes (2 GO processes and 2 STOP processes) is parameterized by a mean rate $\mu$ and variance $\sigma$ about this rate, leading to a total of eight parameters.

We first consider how to obtain rate estimates for the GO processes. Rates relate to observed RTs in a straightforward manner: a distribution of rates is obtained simply by taking the reciprocals of observed RTs [(Carpenter and Williams 1995), Fig. 7, *B* and *C*]. Thus for *model 1,* obtaining ($\mu$, $\sigma$) for the rates of gaze and head GO processes involves taking the reciprocal of observed RTs on control trials and obtaining the maximum likelihood estimates for ($\mu$, $\sigma$) of this data using the "mle" function in the Matlab Statistics Toolboxes (Fig. 7, *B* and *C*; this method assumes that GO and STOP rates are drawn from a Gaussian distribution).

Estimating the rates for the STOP processes involves determining the STOP rate distribution that provides the best match to the observed proportion of noncanceled and canceled trials. Following the method of Kornylo and colleagues (2003), we used a nonlinear minimization technique (the "fminsearch" function in Matlab, which implements the Nelder-Mead simplex method) to determine the most likely ($\mu$, $\sigma$) for the STOP rate distribution, given the previously determined GO rate distribution and observed inhibition functions. Figure 7, *B–D*, displays a candidate distribution for the STOP process, shown as a RT distribution in Fig. 7*B*, a rate distribution in Fig. 7*C*, and a cumulative rate distribution in Fig. 7*D*. We derived a similar cumulative rate distribution for the GO process and inverted so that it had the opposite orientation as the STOP cumulative rate distribution (Fig. 7*D*). The intersection between these two curves (arrow in Fig. 7*D*) indicates the expected proportion of noncanceled trials. By altering the ($\mu$, $\sigma$) of the STOP rate distribution, it is possible to determine parameters that minimize the difference between the expected and observed proportion of noncanceled trials.

The preceding procedure applies only to the case in which the SSD equals 0. To account for a variety of SSDs, which effectively delay the onset of the STOP process, it is necessary to shift the candidate STOP RT distribution (in Fig. 7*B*) rightward by the SSD and then proceed as in the preceding text, deriving a new STOP rate distribution from the reciprocals of the shifted STOP RT distribution. In Fig. 7*E*, we provide a series of STOP rate distributions calculated after shifting the STOP RT distribution for the full set of SSDs. Note that adding the SSD to the STOP RT distribution shifts the STOP rate distribution to lower values with progressively larger effects on higher rates.

The points of intersection in Fig. 7*E* provide the predicted frequencies of noncanceled trials for the full set of SSDs, given the candidate STOP rate distribution, which can be compared with the observed frequencies trials provided by the inhibition functions (e.g., Fig. 4). To derive the STOP rate parameters that best fit the observed data, we again followed the methods of Kornylo and colleagues (2003). At each SSD, we calculated the likelihood of the observed proportion of noncanceled trials based on the binomial distribution, given the frequency predicted by the intersection of the GO and STOP rate distributions. We then determined a cost for the candidate STOP rate distribution, calculated as the sum of the negative log of each likelihood value across all SSDs. The cost is a single positive value that is smaller for candidate STOP rate distributions that better match the data, and it is this cost that is minimized by the nonlinear minimization technique. Once it has converged on a solution, this method provides estimates of the ($\mu$, $\sigma$) for the

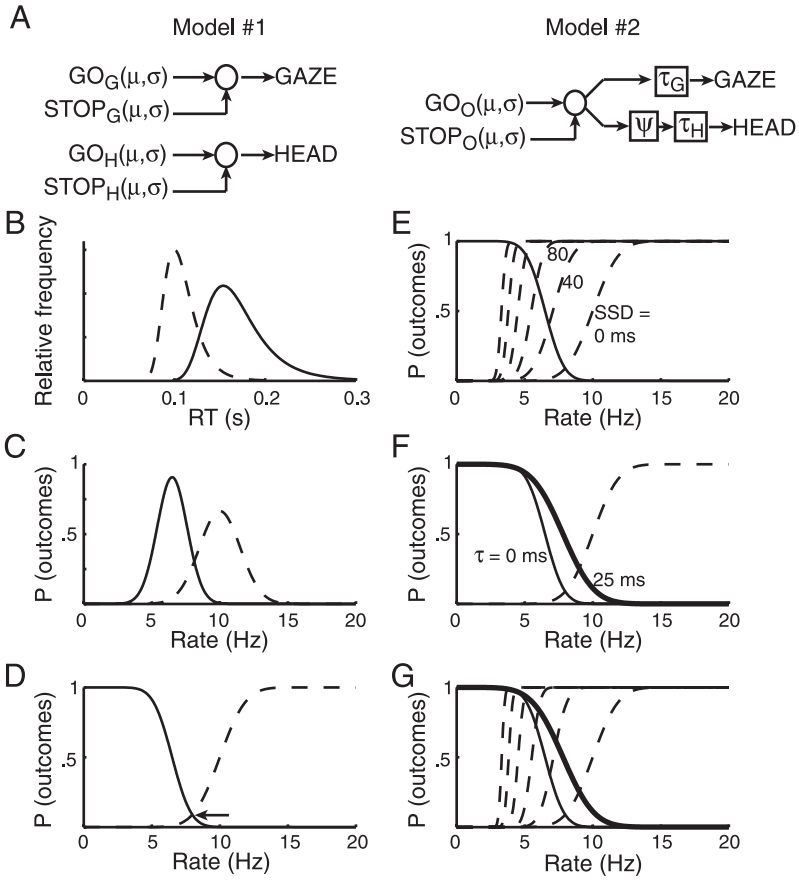


FIG. 7. Depiction of the proposed extensions to the race models, and of the method of Kornylo and colleagues (2003) for estimating the rate parameters of GO and STOP processes. *A*: schematic diagram of 2 alternative extensions of the race model to explain our data. *Model 1* assumes that gaze shifts and head movements have independent GO and STOP processes. The Gaussian distributions of these rates (the reciprocal of the RT distributions) are parameterized by a mean ($\mu$) and SD ($\sigma$). *Model 2* assumes that gaze shifts and head movements are controlled by a single race of "oculomotor" GO and STOP processes. Further, the gaze and head branches contain a ballistic interval ($\tau$) that is not under inhibitory control. Finally, the head branch is activated at a different threshold ($\psi$) than the gaze branch; if $\psi < 1$, then the head branch has a lower activation threshold than the gaze branch. *B*: RT distributions for the GO process (obtained from measured RTs, solid line) and for a candidate STOP process (dashed line). *C*: the same GO and STOP processes plotted as rate distributions obtained by taking the reciprocals of the RT distributions. These rate distributions form Gaussian distributions that can be characterized by $\mu$ and $\sigma$. *D*: GO and STOP processes plotted as cumulative distribution functions. The GO rate distribution has been inverted. The point of intersection between these 2 curves (horizontal arrow) indicates the frequency of noncanceled trials predicted by these GO and STOP processes. *E*: the set of STOP rate distributions obtained by adding the set of SSDs used in these experiments. Each shifted STOP rate distribution is obtained by adding the SSD to the STOP RT distribution shown in *B* and proceeding as above. The GO rate distribution is the same as before. *F*: introducing a terminal ballistic interval (here 25 ms) has the effect of shifting the GO RT distribution in *B* toward lower values and hence the cumulative rate distribution to higher values (thick solid line). The STOP rate distribution is the same as in *D*. *G*: introducing the terminal ballistic interval alters the intersection points between the GO rate distribution and the set of shifted STOP rate distributions (here, the same as in *E*). A different candidate STOP process, shifted rightward toward higher rates, would be required to attain the same intersection points as in *E*.

STOP rate distribution that best fits the observed inhibition functions.

For *model 1* (Fig. 7*A*), we simulated separate race models for gaze and head data. For each subject, the four rate parameters for the gaze and head GO processes were determined directly from the empirical control RT distributions. The four rate parameters for the gaze and head STOP processes were then determined using the technique described in the preceding text. As shown in Fig. 8, the frequency of noncanceled trials for both gaze shifts and head movements predicted by *model 1* provided a good qualitative match to the observed inhibition functions. The eight parameters for this model are shown in Table 2. The mean ($\mu$) GO and STOP rates derived for gaze shifts are not statistically different from similarly derived values quoted for head-fixed saccades in humans [(Kornylo et al. 2003) Wilcoxon rank-sum test, $P > 0.5$ for both GO and STOP rates].

We then tested a second version of the race model (Fig. 7*A*, *model 2*) based on the dual-threshold hypothesis. In this version, control of gaze shifts and head movements are dictated by the outcome of a single race between "oculomotor" GO and STOP processes. The final motor pathways for both gaze shifts and head movements contain a ballistic interval ($\tau$) that is not under inhibitory control (Osman et al. 1986). A final feature is that the branch controlling head movements is activated when the oculomotor GO process reaches at a lower threshold ($\psi$), which is simply a fraction relative to the threshold for initiating gaze shifts (i.e., values $<1$ imply that head threshold is less than gaze threshold; values $>1$ imply the opposite). A lower threshold is consistent with neurophysiological observations that head movements can be initiated without gaze shifts (Corneil and Munoz 1999; Corneil et al. 2002a,b) and is necessary in this architecture to permit occurrences of head movements without gaze shifts. *Model 2* is characterized by seven parameters (4 rate parameters, 2 ballastic intervals, and 1 threshold).

Following the same methodology as in the preceding text (Kornylo et al. 2003), the introduction of a ballistic interval effectively shifts the GO RT distribution to lower values, reducing the portion of the RT under inhibitory control. This consequently shifts the GO rate distribution to higher values (Fig. 7*F*). A lower threshold ($\psi < 1$) has a similar consequence by also reducing the portion of the head movement RTs under inhibitory control, in effect allowing head movements to be initiated earlier relative to target onset.

For *model 2,* we first estimated rate parameters for the oculomotor GO process. To do this, we combined estimates of oculomotor RTs based on gaze and head RTs from control trials. Oculomotor RTs based on gaze shifts were estimated by subtracting a candidate gaze ballastic interval ($\tau_G$) from the distribution of gaze shift RTs. Oculomotor RTs based on head movements were estimated by subtracting a candidate head ballastic interval ($\tau_H$) from head movement RTs and further dividing these values by the fraction of the lower threshold ($\psi$). For $\psi < 1$, this division effectively increases the estimates of the oculomotor RTs based on head movements, which is necessary to account for the lower head movement threshold. These head and gaze estimates for oculomotor RTs were then combined, and reciprocals of this RT distribution taken to derive the rate parameters of the oculomotor GO process as in the preceding text.

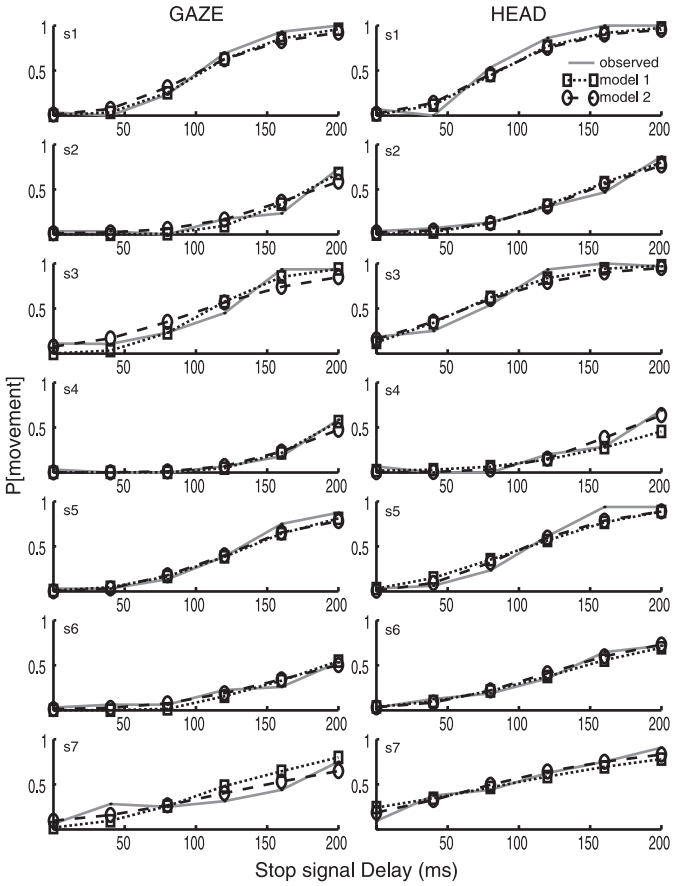


FIG. 8. Comparison of empirical gaze and head inhibition functions (solid gray lines) with inhibition functions generated by *model 1* (squares, dotted lines) and *model 2* (circles, dashed lines).

Using a candidate STOP rate distribution and this derived GO rate distributions (shifted by $\tau_G$ for gaze shifts and by $\tau_H$ and $\psi$ for head movements), we employed the same techniques described in the preceding text to obtain maximum likelihood estimates of the parameters for *model 2*. In estimating the proportion of noncanceled head movements, we accounted for $\psi$ by shifting GO rates to higher values (as a consequence of lowering oculomotor GO RTs). As shown in Fig. 8, the frequency of noncanceled trials for gaze shifts and head movements predicted by *model 2* also provided a good qualitative fit to the observed inhibition functions. The parameters for these fits are provided in Table 2. For all seven subjects, the estimated ballistic interval for gaze shifts averaged 26.7 ± 6.7 ms (range: 20.6–38.1). The estimated ballistic interval for head movements was 89.5 ± 10.7 ms (range: 73.5–99.9). Further, $\psi$ was always <1 (mean: 0.84 ± 0.07, range: 0.73–0.90), implying that the threshold for activating head movements was less than gaze shifts for all subjects.

A quantitative analysis demonstrated that both models fit the empirical data very well. We first analyzed the proportion of noncanceled trials predicted by each model versus the observed data and found that both models fit the data reasonably well [for both models across all subjects (28 comparisons), Kolgomorov-Smirnov test between predicted and observed rates of noncanceled gaze shifts or head movements, $P > 0.3$]. To compare the fits of the models, we calculated the sum of squares of the difference between predicted and estimated rates of noncanceled gaze shifts and head movements, and revealed no significant difference in model performance (Wilcoxon signed-rank test, $P$ 0.45 for comparative model performance for both gaze shifts and head movements).

As a final step to examine the validity of these estimated rates, we compared the gaze and head SSRTs derived from *models 1* and *2* to those estimated from the integration and mean methods presented (Table 3). Gaze and head SSRTs are derived from the maximum likelihood estimates by simply taking the reciprocal of the appropriate mean STOP rate (*model 1*) or by adding the appropriate ballistic interval to the reciprocal of the mean oculomotor STOP rate (*model 2*). A number of patterns deserve mention. First, within a given subject, the various SSRT estimates were fairly consistent with estimates differing on average by ~14 ms for gaze SSRTs (range: 0–52 ms) and ~18 ms for head SSRTs (range: 2–55 ms). Second, the estimates for gaze SSRTs did not depend on the method used [1-way repeated-measures ANOVA, $F(1,3,18) = 0.46$, $P = 0.71$]. Third, the estimates for head SSRTs did depend on the method used, being longest when derived by the integration method, and shortest when derived by model 2 [$F(1,3,18) = 3.25$, $P = 0.05$]. Our overall impression is that these modeling efforts do a very good job describing the observed behavior.

## DISCUSSION

To our knowledge, this is the first study to investigate how humans countermand eye-head gaze shifts. Previous head-restrained recording studies support the notion that saccade control is dictated by GO and STOP processes racing to a critical activation threshold (Hanes and Carpenter 1999; Hanes and

TABLE 2. *Maximum likelihood estimates of the parameters for two versions of the race model*

| | Model 1 | | | | Model 2 | | | | |
|---|---|---|---|---|---|---|---|---|---|
| Subject | Gaze GO rate | Head GO rate | Gaze STOP rate | Head STOP rate | Oculomotor GO rate | Oculomotor STOP rate | $\tau$ Gaze, ms | $\tau$ Head, ms | Head pathway threshold, $\psi$ |
| *s1* | 4.94 ± 0.78 | 3.97 ± 0.58 | 10.42 ± 0.66 | 5.97 ± 0.12 | 5.60 ± 1.19 | 13.40 ± 1.48 | 32.8 | 78.4 | 0.90 |
| *s2* | 3.47 ± 0.48 | 2.90 ± 0.36 | 8.95 ± 0.41 | 4.97 ± 0.21 | 3.68 ± 0.61 | 11.90 ± 2.30 | 21.5 | 98.3 | 0.88 |
| *s3* | 4.61 ± 0.68 | 4.04 ± 0.56 | 9.33 ± 0.55 | 5.39 ± 0.35 | 4.93 ± 1.15 | 10.91 ± 2.18 | 28.2 | 73.5 | 0.78 |
| *s4* | 3.39 ± 0.53 | 2.89 ± 0.43 | 9.53 ± 0.28 | 7.58 ± 1.19 | 3.66 ± 0.70 | 14.72 ± 2.13 | 20.6 | 97.4 | 0.90 |
| *s5* | 3.52 ± 0.55 | 3.25 ± 0.60 | 6.86 ± 0.50 | 4.80 ± 0.12 | 4.08 ± 0.97 | 8.56 ± 0.30 | 38.1 | 83.9 | 0.89 |
| *s6* | 3.50 ± 0.75 | 2.93 ± 0.60 | 9.01 ± 0.17 | 5.17 ± 0.36 | 3.58 ± 1.06 | 12.60 ± 2.15 | 21.3 | 99.9 | 0.78 |
| *s7* | 3.75 ± 0.85 | 3.22 ± 0.72 | 6.98 ± 0.42 | 4.69 ± 0.84 | 3.86 ± 1.28 | 9.72 ± 2.34 | 24.0 | 94.9 | 0.73 |
| Mean | 3.89 ± 0.63 | 3.32 ± 0.50 | 8.73 ± 1.33 | 5.51 ± 1.01 | 4.20 ± 0.77 | 11.7 ± 2.13 | 26.7 ± 6.7 | 89.5 ± 10.7 | 0.84 ± 0.07 |

Rate parameters have units of hertz and are given as means ± SD corresponding to the ($\mu$,$\sigma$) symbols, respectively, in Fig. 7. $\tau$ denotes the ballistic interval preceding gaze shifts or head movements. The threshold for the head pathway ($\psi$) is simply a fraction of the gaze pathway and has no units.

TABLE 3. *Four estimates each for gaze and head SSRTs*

| | Gaze SSRTs | | | | | Head SSRTs | | | | |
|---|---|---|---|---|---|---|---|---|---|---|
| Subject | Integration method | Mean method | *Model 1* | *Model 2* | Average | Integration method | Mean method | *Model 1* | *Model 2* | Average |
| *s1* | 101 ± 3 | 82 | 96 | 107 | 97 | 178 ± 2 | 156 | 167 | 153 | 164 |
| *s2* | 121 ± 17 | 122 | 112 | 105 | 115 | 203 ± 17 | 191 | 201 | 182 | 194 |
| *s3* | 137 ± 41 | 85 | 107 | 120 | 112 | 197 ± 27 | 158 | 185 | 165 | 176 |
| *s4* | 103 ± 4 | 122 | 105 | 89 | 105 | 177 ± 13 | 187 | 132 | 165 | 165 |
| *s5* | 152 ± 8 | 146 | 146 | 155 | 150 | 205 ± 6 | 193 | 208 | 201 | 202 |
| *s6* | 107 ± 19 | 138 | 111 | 101 | 114 | 214 ± 19 | 225 | 194 | 179 | 203 |
| *s7* | 140 ± 38 | 141 | 143 | 127 | 138 | 227 ± 23 | 217 | 213 | 198 | 214 |
| Mean | 123 ± 19 | 119 ± 19 | 117 ± 19 | 115 ± 22 | 119 ± 19 | 200 ± 15 | 190 ± 26 | 186 ± 28 | 178 ± 18 | 188 ± 20 |

For the maximum likelihood estimate models, we either took the reciprocal of the mean STOP rate for gaze or head (model 1) or added the appropriate gaze ballistic interval to the reciprocal of the mean oculomotor STOP rate (model 2). All stop-signal reaction times (SSRTs) reported in milliseconds.

Schall 1996; Hanes et al. 1998; Paré and Hanes 2003). There are three main findings in this report. First, the control of the gaze axis with the head unrestrained approximates that with the head restrained: our derived gaze SSRTs of ~120 ms compares favorably to previous results from head-restrained humans with foveal stop-signals (Asrress and Carpenter 2001; Cabel et al. 2000; Hanes and Carpenter 1999; Kornylo et al. 2003; Ozyurt et al. 2003). Second, for all subjects, we observed a novel response sequence wherein the head moved in the direction of the target even though gaze remained stable and never observed the converse sequence where gaze moved while the head remained stable. Third, for all subjects, head SSRTs were substantially longer than gaze SSRTs. These results are inconsistent with a race model of the simple form assumed for head-restrained saccades that predict head movements only in conjunction with gaze shifts. In this discussion, we consider the implications of the observed behaviors on contemporary notions of oculomotor control, compare the merits of two alternative extensions to the race model, and make predictions about the neural activity which we believe generates the observed behaviors.

### *Head movements are committed to before gaze shifts*

We observed two types of gaze shifting responses on STOP trials: subjects were either able to cancel an eye-head gaze shift or not. Such behaviors, and the SSRTs estimated for gaze shifts, are essentially identical to the patterns observed with the head restrained, suggesting that neither head restraint nor the large eccentricity employed in this study imparted a major effect on the neural processes controlling the gaze axis.

More importantly, there were two types of appropriately suppressed gaze shifts on STOP trials: those in which the head remained still and those in which the head moved to the target. The latter movement sequence is perhaps the most surprising aspect of our data. The metrics and incidence of head movements without gaze shifts are substantial: they frequently exceeded 10° and occurred at a relatively high frequency (about one-third that of noncanceled gaze shifts; Table 1). Although our measurement techniques precluded a close dynamic analysis of such head movements (e.g., acceleration profiles), they resemble head movements produced in a distractor task in which the head oriented in one direction even though an ensuing gaze shift went in the other (Corneil and Munoz 1999).

Sequences in which the head moves while gaze remains stable indicate a degree of independence in the control of gaze shift and head-movement initiation. The timing of the neuromuscular commands that underlie this independence is all the more surprising given the inertial lag inherent to head motion, which ranges ~55 ms for the large horizontal orienting head movements required here (Zangemeister and Stark 1982). Our findings underscore the value of the countermanding task as a tool for assessing the response control capabilities of the oculomotor system. That subjects are frequently able to suppress gaze shifts but not head movements, not the other way around, indicates that a commitment to a head movement is made before a commitment to a gaze shift.

### *Can race models explain the observed behaviors?*

Clearly a simple race model of the type envisaged for controlling head-restrained saccades cannot explain the observed behavioral sequences. However, this shortcoming need not discredit race models entirely. Indeed, many aspects of the observed behaviors are consistent with race models in general. For example, RTs of noncanceled gaze or head movements were well predicted by the RTs in control trials that started before the sum of the SSD and SSRT (Fig. 6). Given the close coupling between gaze and head RTs (Fig. 2), similar lines of logic can be followed to explain why head movement RTs were shortest when made during noncanceled gaze shifts, longer for head-only movements on STOP trials, and longer still for eye-head gaze shifts on control trials (Table 1). Finally, if one accepts that the race to threshold dictates movement initiation only, then the tradeoff between noncanceled movement amplitude and SSD (Fig. 3) is also consistent with race models as noncanceled movements proceed farther for longer SSDs before being arrested by the STOP process. Tradeoffs between noncanceled movement amplitude and SSD have been reported in some saccade-countermanding studies (Colonius et al. 2001; Ozyurt et al. 2003; Paré and Hanes 2003) but not others (Hanes and Schall 1995; Kornylo et al. 2003), likely because of differences in target eccentricity. The large target eccentricity used here necessitate long movement durations, providing more time for interactions between the STOP process and the ongoing movement. Indeed, the amplitude-SSD relationships reported here resemble those described earlier in double-step and distractor experiments (Becker and Jurgens

1979; Corneil et al. 1999; Lisberger et al. 1975; Viviani and Swensson 1982).

Led by these parametric relationships, we proposed two alternative extensions (Fig. 7*A*) to the race model used for saccade control. Model 1 simply posits that two races, independent but conducted in parallel, underlie the control of gaze shifts and head movements. In contrast, *model 2* (implementing the dual threshold hypothesis) posits that a single race dictates oculomotor control and that the outcome of this race is relayed through separate gaze and head branches. Importantly, although both branches include terminal ballistic intervals not subject to inhibitory control,[1] the essential feature of *model 2* is that the head branch is activated when the GO process reaches a lower threshold compared with that required to initiate gaze shifts. Using the maximum likelihood techniques presented recently (Kornylo et al. 2003), both models were able to simulate the observed behaviors fairly well (Fig. 8). Moreover, the gaze and head SSRTs estimated from these extensions compared favorably with those calculated in more conventional fashions (Table 3). We are therefore confident that processes general to race models generated the observed behaviors.

### *Do separate or conjoined races underlie control of eye-head gaze shifts?*

Although the results of our simulations (Fig. 8) provide no justification for favoring one race model extension over the other, a further series of considerations apply. For example, one could argue that *model 2* is "better" because it requires fewer parameters than *model 1*. Although this line of reasoning may be relevant from a computational perspective, the neural implementation of gaze and head control need not be so constrained.

Another criticism against *model 1* is that it, as presented in Fig. 7*A*, predicts occurrences of noncanceled gaze shifts without head movements (i.e., if the gaze GO process reaches threshold, but the head GO process does not). Such movement sequences were never observed in the current experiments. However, this criticism can easily be met by imaging a scenario wherein large-amplitude gaze shifts are obligatorily coupled with head movements. Further, there was a high degree of coupling between eye (gaze) and head RT that is not captured by *model 1* (Fig. 2).

The most compelling arguments favoring *model 2* over *model 1* come from neuroanatomical and neurophysiological findings of the oculomotor system. The bulk of evidence suggest that the control of orienting gaze shifts and head movements are linked down to the level of the superior colliculus [SC; for review see (Scudder et al. 2002)] and do not display the anatomical segregation seen, for example, in the systems controlling eye and hand motion. Neural activity within the SC represents the desired gaze shift rather than the underlying components of the eye or head (Freedman and Sparks 1997). Head-restrained studies demonstrate that movement-related neurons within the SC discharge less when saccades are successfully countermanded, suggesting that saccades are triggered when these neurons reach a critical activation level [(Paré and Hanes 2003); similar activity profiles are seen in the frontal eye fields (Hanes and Schall 1996)]. In head-unrestrained preparations, this critical activation level likely determines whether gaze shifts will be countermanded or not. This leaves unanswered the generation of head movements without gaze shifts.

A number of recent results suggest that the role of the SC in orienting is not as simple as a single critical activation level would suggest. First, although high levels of electrical stimulation delivered to the SC drive naturally appearing eye-head gaze shifts (Freedman et al. 1996; Klier et al. 2001), lower levels of stimulation current can recruit neck muscles and head movements without gaze shifts (Corneil et al. 2002a,b; Pélisson et al. 2001). Second, the presentation of a bright visual target recruits a time-locked burst of activity on ipsilateral neck muscles, resembling the visual burst of activity in the SC, regardless of the ensuing saccadic reaction time (Corneil et al. 2004). Third, preliminary results demonstrate that the level of neck EMG activity evoked by very short-duration SC stimulation covaries with the known variations of low-frequency SC activity during a gap task similar to the one employed here (Corneil et al. 2000). Together, these results suggest that SC activity below the threshold for initiating gaze shifts can nevertheless recruit neck muscles, culminating in observable head movements if given enough time to overcome the head's inertia. We believe that the omni-pause neurons, a group of neurons that tightly constrain gaze shift generation [see (Scudder et al. 2002) for review], play a crucial role in this scenario by preventing such subthreshold SC activity from initiating gaze shifts without controlling the initiation of head movements.

Relating this mechanism back to the countermanding task, we propose that eye-head gaze shifts are launched toward the target if activity exceeds a high threshold, as discussed in the preceding text. If not, gaze remains stable and the VOR remains engaged to compensate for any head movement. The question of whether a head movement is canceled or not then becomes whether SC activity exceeds a lower threshold of activity. For the first time, our modeling simulations allow us to ascribe a value to this lower threshold, suggesting that head movements are initiated if the GO process reaches a level ~85% of the activation level controlling gaze shifts. Whether this level relates directly to neural phenomena awaits neurophysiological experiments in head-unrestrained subjects.

### *Longer ballistic interval precedes head movements versus gaze shifts*

If one accepts our supposition that a unified race within the oculomotor system to two thresholds determines the initiation of gaze shifts and head movements, then our findings regarding the comparative gaze and head SSRTs seem incongruous. If gaze and head movements are indeed controlled by unified GO and STOP processes, then head SSRTs should be the same as gaze SSRTs. While true, this perspective neglects the contribution of a ballistic interval, which is the "point-of-no-return"

[1] While the terminal ballistic intervals $\tau_G$ and $\tau_H$ are necessary for *model 2* to generate differences in comparative gaze and head RTs, such intervals could have been incorporated into *model 1*. As discussed in Kornylo et al. (2003), the effect of introducing ballistic intervals (shortening the portion of the GO process under inhibitory control) can be compensated for by shifting the STOP process to higher rates, and the same predicted inhibition functions can still be derived. Because the gaze and head pathways in *model 1* are completely independent, terminal ballistic intervals are not strictly necessary, and hence we have excluded them for the sake of simplicity.

interval beyond which movement initiation cannot be prevented (Osman et al. 1986). The biomechanics of head and eye motion (eye motion typically initiates gaze shifts) are quite different: the head in particular is characterized by a far greater inertia (Zangemeister and Stark 1981), and skeletal muscles take longer to develop forces following recruitment than their extraocular counterparts (Barmack et al. 1971; Botterman et al. 1986). For example, even though neck muscles are recruited 10–35 ms after SC stimulation (Corneil et al. 2002a), head motion is usually initiated between 30 and 100 ms later and is highly dependent on the location and parameters of stimulation (Corneil et al. 2002b; Freedman et al. 1996). In contrast, activation of premotor burst neurons lead eye saccades by ~10 ms (Scudder et al. 2002). Thus the time from muscle recruitment to movement onset, which constitutes at least part of the ballistic interval, is longer for head movements than gaze shifts, and likely explains much of the ~70–80 ms difference in head versus gaze SSRT.

Our estimates for the ballistic intervals in *model 2* are in good agreement with the known physiology of the oculomotor system. The gaze ballistic interval was estimated to be ~25 ms, and although this is much shorter and less variable than that estimated previously for saccadic eye movements in humans (Kornylo et al. 2003), it is in good agreement with the 20 ms by which the burst in SC neurons precedes saccade onset in monkeys (Munoz and Wurtz 1995; Sparks 1978). Our estimates of the head ballistic interval ranged ~90 ms or ~65 ms longer than the gaze ballistic interval. Assuming that data from monkeys is applicable to humans, much of the ~90 ms interval is humans can be attributed to the lag between SC activation and head movement onset.

### *What constitutes response control for an inertial body segment?*

In the countermanding task, the question usually being considered is whether a given body segment moves or not. For saccadic eye movements, control depends likely on whether signals are issued to the eye plant; the mechanics of eye motion are such that only very small levels of force are required to move the eyes (Goldberg et al. 1998). This situation is quite different for an object, like the head, characterized by a large inertial load. This inertial load is only part of the complex linkage between the earliest neuromuscular event (accessible via electromyographic recordings), force development, and movement onset (Zajac and Gordon 1989). Indeed, lag due to the inertial load, as well other nonlinearities in force development, may provide a longer window of opportunity for the STOP process to prevent movement production. Studies of countermanding squeezing movements, for example, demonstrate instances where muscle recruitment is initially produced but inhibited in time to prevent an overt response that must exceed a certain force (De Jong et al. 1990). Clearly in this case, the GO process won the race to initiate neuromuscular events but did not win the race by long enough to permit evolution of a quantifiable response. Thus when considering control of an inertial body segment, it would appear important to consider not only whether the GO process exceeds an activation threshold but also for how long this activation threshold is exceeded.

A parallel between these findings can be drawn to the control of head motion; in our task, there may well have been instances where neck muscles were recruited even though the head ultimately remained stable because of insufficient force generation. Given the observation that the onset of a bright light leads to lateralized neck muscle recruitment (Corneil et al. 2004), it is indeed probable that there was lateralized neck muscle recruitment well before head movement onset, but whether this occurs on STOP trials when both gaze and head movements were canceled is unknown. Recordings of neck muscle activity would seem to be required for a number of other questions as well. For example, can inhibition functions for neck muscle recruitment be generated, and how do neck muscle SSRTs compare with head SSRTs and the ballistic interval preceding head motion? Further, what is the neuromuscular signature associated with stopping the head: are antagonist muscles recruited, are agonist muscles simply silenced, or are agonist and antagonist muscles co-contracted? This latter question is completely open, and indeed it is possible that the STOP process will recruit different neuromuscular patterns depending on how far along the GO process has evolved prior to movement initiation. The combination of muscle recruitment recordings with the recording of neural activity in areas such as the SC will likely provide further insights into the brain stem mechanisms ultimately dictating head movement control and may generalize to other inertial movement systems like the limb.

### *Conclusions*

We have studied how humans countermand eye-head gaze shifts and demonstrated that humans frequently generate three response profiles when instructed to try to cancel a planned eye-head gaze shift. These results could not have been predicted from head-restrained countermanding studies but are parsimonious with a number of recent electrophysiological findings that suggest that low levels of SC activity can drive head movements without gaze shifts. These brain stem mechanisms appear to, somewhat paradoxically, permit the CNS to commit to a head movement while still having enough time to abort a planned gaze shift. It is possible that this mechanism has evolved given the paramount importance of retinal stability for foveal vision or because of the sluggish biomechanics of the head. Alternatively, our results may testify to a brain stem mechanism that specifies the head movement trajectory before the gaze shifts begins to optimize the final position of the eyes within the head in different behavioral contexts (Crawford and Guitton 1997; Oommen et al. 2004; Tweed et al. 1998). It remains to be seen whether these results are specific for the oculomotor system or generalize to other movement systems such as reaching or eye-hand coordination.

ACKNOWLEDGMENTS

We thank Dr. S. Everling and B. Chapman for comments on earlier versions of this manuscript.

GRANTS

This research was supported by a grant from the Canadian Institutes on Health Research (MOP 64202), start-up funds provided by the University of Western Ontario, and infrastructure support from the Canadian Foundation for Innovation and the Ontario Innovation Trust.

REFERENCES

**Asrress KN and Carpenter RH.** Saccadic countermanding: a comparison of central and peripheral stop signals. *Vision Res* 41: 2645–2651, 2001.

**Barmack NH, Bell CC, and Rence BG.** Tension and rate of tension development during isometric responses of extraocular muscle. *J Neurophysiol* 34: 1072–1079, 1971.

**Becker W and Jurgens R.** An analysis of the saccadic system by means of double step stimuli. *Vision Res* 19: 967–983, 1979.

**Botterman BR, Iwamoto GA, and Gonyea WJ.** Gradation of isometric tension by different activation rates in motor units of cat flexor carpi radialis muscle. *J Neurophysiol* 56: 494–506, 1986.

**Boucher L, Stuphorn V, Logan GD, Palmeri TJ, and Schall JD.** Dissecting the stop process: eye-hand coordination in a stop task. *Soc Neurosci Abstr* 30: 313.6. 2004.

**Cabel DW, Armstrong IT, Reingold E, and Munoz DP.** Control of saccade initiation in a countermanding task using visual and auditory stop signals. *Exp Brain Res* 133: 431–441, 2000.

**Carpenter RH and Williams ML.** Neural computation of log likelihood in control of saccadic eye movements. *Nature* 377: 59–62, 1995.

**Colonius H, Ozyurt J, and Arndt PA.** Countermanding saccades with auditory stop signals: testing the race model. *Vision Res* 41: 1951–1968, 2001.

**Corneil BD, Hing CA, Bautista DV, and Munoz DP.** Human eye-head gaze shifts in a distractor task. I. Truncated gaze shifts. *J Neurophysiol* 82: 1390–1405, 1999.

**Corneil BD and Munoz DP.** The influence of auditory and visual distractors on human orienting gaze shifts. *J Neurosci* 16: 8193–8207, 1996.

**Corneil BD and Munoz DP.** Human eye-head gaze shifts in a distractor task. II. Reduced threshold for initiation of early head movements. *J Neurophysiol* 82: 1406–1421, 1999.

**Corneil BD, Olivier E, and Munoz DP.** Features of the drive to dorsal neck muscles from the primate superior colliculus. *Soc Neurosci Abstr* 26: 109.7. 2000.

**Corneil BD, Olivier E, and Munoz DP.** Neck muscle responses to stimulation of monkey superior colliculus. I. Topography and manipulation of stimulation parameters. *J Neurophysiol* 88: 1980–1999, 2002a.

**Corneil BD, Olivier E, and Munoz DP.** Neck muscle responses to stimulation of monkey superior colliculus. II. Gaze shift initiation and volitional head movements. *J Neurophysiol* 88: 2000–2018, 2002b.

**Corneil BD, Olivier E, and Munoz DP.** Visual responses on neck muscles reveal selective gating that prevents express saccades. *Neuron* 42: 831–841, 2004.

**Crawford JD and Guitton D.** Primate head-free saccade generator implements a desired (post-VOR) eye position command by anticipating intended head motion. *J Neurophysiol* 78: 2811–2816, 1997.

**De Jong R, Coles MG, Logan GD, and Gratton G.** In search of the point of no return: the control of response processes. *J Exp Psychol Hum Percept Perform* 16: 164–182, 1990.

**Dorris MC and Munoz DP.** A neural correlate for the gap effect on saccadic reaction times in monkey. *J Neurophysiol* 73: 2558–2562, 1995.

**Freedman EG, and Sparks DL.** Activity of cells in the deeper layers of the superior colliculus of the rhesus monkey: evidence for a gaze displacement command. *J Neurophysiol* 78: 1669–1690, 1997.

**Freedman EG, Stanford TR, and Sparks DL.** Combined eye-head gaze shifts produced by electrical stimulation of the superior colliculus in rhesus monkeys. *J Neurophysiol* 76: 927–952, 1996.

**Galiana HL and Guitton D.** Central organization and modeling of eye-head coordination during orienting gaze shifts. *Ann NY Acad Sci* 656: 452–471, 1992.

**Goldberg SJ, Meredith MA, and Shall MS.** Extraocular motor unit and whole-muscle responses in the lateral rectus muscle of the squirrel monkey. *J Neurosci* 18: 10629–10639, 1998.

**Hanes DP and Carpenter RH.** Countermanding saccades in humans. *Vision Res* 39: 2777–2791, 1999.

**Hanes DP, Patterson WF, and Schall JD.** Role of frontal eye fields in countermanding saccades: visual, movement, and fixation activity. *J Neurophysiol* 79: 817–834, 1998.

**Hanes DP and Schall JD.** Countermanding saccades in macaque. *Vis Neurosci* 12: 929–937, 1995.

**Hanes DP and Schall JD.** Neural control of voluntary movement initiation. *Science* 274: 427–430, 1996.

**Ito S, Stuphorn V, Brown JW, and Schall JD.** Performance monitoring by the anterior cingulate cortex during saccade countermanding. *Science* 302: 120–122, 2003.

**Klier EM, Wang H, and Crawford JD.** The superior colliculus encodes gaze commands in retinal coordinates. *Nat Neurosci* 4: 627–632, 2001.

**Kornylo K, Dill N, Saenz M, and Krauzlis RJ.** Cancelling of pursuit and saccadic eye movements in humans and monkeys. *J Neurophysiol* 89: 2984–2999, 2003.

**Lisberger SG, Fuchs AF, King WM, and Evinger LC.** Effect of mean reaction time on saccadic responses to two-step stimuli with horizontal and vertical components. *Vision Res* 15: 1021–1025, 1975.

**Logan GD.** On the ability to inhibit thought and action: a users' guide to the stop-signal paradigm. In: *Inhibitory Processes in Attention, Memory and Language,* edited by Dagenbach D and Carr H. Kent: Academic, 1994, p. 189–239.

**Logan GD and Cowan WB.** On the ability to inhibit thought and action: a theory of an act of control. *Psychol Rev* 91: 295–327, 1984.

**Logan GD and Irwin DE.** Don't look! Don't touch! Inhibitory control of eye and head movements. *Psychon Bull Rev* 7: 107–112, 2000.

**Mirabella G, Pani P, and Ferraina S.** Countermanding reaching in monkeys (*Macaca mulatta*) and humans. *Soc Neurosci Abstr* 30: 211.4. 2004.

**Munoz DP and Wurtz RH.** Saccade-related activity in monkey superior colliculus. I. Characteristics of burst and buildup cells. *J Neurophysiol* 73: 2313–2333, 1995.

**Oommen BS, Smith RM, and Stahl JS.** The influence of future gaze orientation upon eye-head coupling during saccades. *Exp Brain Res* 155: 9–18, 2004.

**Osman A, Kornblum S, and Meyer DE.** The point of no return in choice reaction time: controlled and ballistic stages of response preparation. *J Exp Psychol Hum Percept Perform* 12: 243–258, 1986.

**Ozyurt J, Colonius H, and Arndt PA.** Countermanding saccades: evidence against independent processing of go and stop signals. *Percept Psychophys* 65: 420–428, 2003.

**Paré M and Hanes DP.** Controlled movement processing: superior colliculus activity associated with countermanded saccades. *J Neurosci* 23: 6480–6489, 2003.

**Pélisson D, Goffart L, Guillaume A, Catz N, and Raboyeau G.** Early head movements elicited by visual stimuli or collicular electrical stimulation in the cat. *Vision Res* 41: 3283–3294, 2001.

**Scudder CA, Kaneko CS, and Fuchs AF.** The brainstem burst generator for saccadic eye movements: a modern synthesis. *Exp Brain Res* 142: 439–462, 2002.

**Sparks DL.** Functional properties of neurons in the monkey superior colliculus: coupling of neuronal activity and saccade onset. *Brain Res* 156: 1–16, 1978.

**Stuphorn V, Taylor TL, and Schall JD.** Performance monitoring by the supplementary eye field. *Nature* 408: 857–860, 2000.

**Tweed D, Haslwanter T, and Fetter M.** Optimizing gaze control in three dimensions. *Science* 281: 1363–1366, 1998.

**Viviani P, and Swensson RG.** Saccadic eye movements to peripherally discriminated visual targets. *J Exp Psychol Hum Percept Perform* 8: 113–126, 1982.

**Zajac FE and Gordon ME.** Determining muscle's force and action in multi-articular movement. *Exer Sport Sci Rev* 17: 187–230, 1989.

**Zangemeister WH and Stark L.** Active head rotations and eye-head coordination. *Ann NY Acad Sci* 374: 540–559, 1981.

**Zangemeister WH and Stark L.** Gaze latency: variable interactions of head and eye latency. *Exp Neurol* 75: 389–406, 1982.